

Competition between commensurate and incommensurate magnetic ordering in Fe_{1+y}Te

D. Parshall,^{1,*} G. Chen,¹ L. Pintschovius,² D. Lamago,^{2,3} Th. Wolf,² L. Radzihovsky,¹ and D. Reznik¹

¹University of Colorado, Department of Physics, Boulder, CO 80309

²Karlsruhe Institut für Technologie, Institut für Festkörperphysik, P.O.B. 3640, D-76021 Karlsruhe, Germany

³Laboratoire Léon Brillouin, CEA-Saclay, F-91191 Gif-sur-Yvette Cedex, France

(Dated: July 19, 2022)

The $\text{Fe}_{1+y}\text{Te}_{1-x}\text{Se}_x$ compounds belong to the family of iron-based high temperature superconductors, in which superconductivity often appears upon doping antiferromagnetic parent compounds. Unlike other Fe-based superconductors (in which the antiferromagnetic order is at the Fermi surface nesting wavevector $[\frac{1}{2}, \frac{1}{2}, 1]$), the $\text{Fe}_{1+y}\text{Te}_{1-x}\text{Se}_x$ parent compound Fe_{1+y}Te orders at a different wavevector, $[\frac{1}{2}, 0, \frac{1}{2}]$. Furthermore, the ordering wavevector depends on y , the occupation of interstitial sites with excess iron; the origin of this behavior is controversial. Using inelastic neutron scattering on $\text{Fe}_{1.08}\text{Te}$, we find incommensurate magnetic fluctuations above the Néel temperature, even though the ordered state is bicollinear and commensurate with gapped spin waves. This behavior can be understood in terms of a competition between commensurate and incommensurate order, which we explain as a lock-in transition caused by the magnetic anisotropy.

PACS numbers: 74.70.Xa 75.30.Gw 64.70.K- 75.40.Gb

Superconductivity in the recently-discovered iron-based superconductors (FeSCs) [1] often appears at high transition temperatures. The common feature of the FeSC materials is a simple square lattice of iron atoms, coordinated with pnictogen or chalcogen atoms forming layers of tetrahedra. The key difference between families is the interplanar layer, which may be a heavy metal ox-

ide, alkaline earth atom, alkali atom, or nothing at all as in the “11” compounds on which we focus here. The parent compounds of most families become orthorhombic and antiferromagnetic (AFM) at low temperatures. These systems are very robust, and superconductivity can be induced by doping with electrons, holes, isoelectronically, or by the application of pressure [2]. Interest in these materials is in large part motivated by their apparently-unconventional high- T_c superconductivity. Because of close proximity to magnetic order, magnetism is believed to be important for superconductivity. There is also intrinsic interest in magnetism in these materials, but it has not been as extensively explored.

The proposed mechanism of superconductivity in the FeSCs that emerged recently [3] comes out of band-theory-based calculations, which show almost perfect nesting between two pockets of the Fermi surface in the parent compounds, which induces the experimentally-observed magnetic order at the nesting wavevector. In this theory, magnetic fluctuations at the same wavevector mediate superconductivity when the nesting has been slightly disturbed.

Although this model explains many experiments, the magnetic order in the $x = 0$ endpoint of the $\text{Fe}_{1+y}\text{Te}_{1-x}\text{Se}_x$ series is a highly unusual “bicollinear” magnetic structure [4], with a wavevector along $\mathbf{q}_{AFM} = [\frac{1}{2}, 0, \frac{1}{2}]$, where neither density function theory (DFT) [5] nor photoemission measurements [6] find any evidence for nesting. The mechanism behind this ordering is one of the main unresolved issues in the effort to understand the FeSCs.

Here we report results of a detailed inelastic neutron scattering (INS) investigation of the region near \mathbf{q}_{AFM} in a high-quality single-crystal sample of $\text{Fe}_{1.08}\text{Te}$. We find strong evidence for competition between commensurate

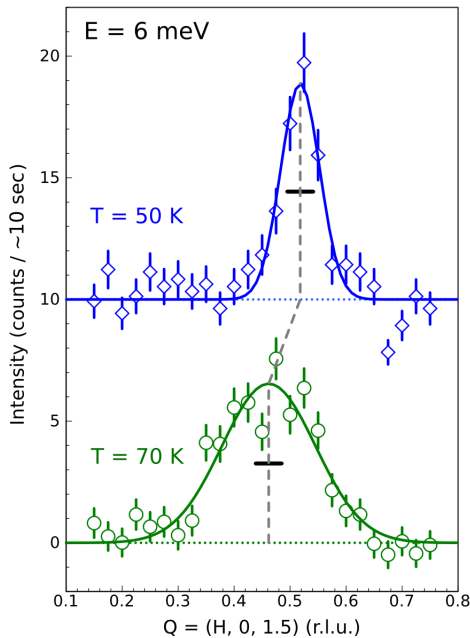


FIG. 1. (color online) Scans through $[\text{H}, 0, \frac{1}{2}]$ with $E = 6$ meV, taken above and below $T_N = 67.5$ K. The black horizontal bar shows the estimated resolution width. The shift of the spin fluctuations from the commensurate to incommensurate position (when warming from the ordered to paramagnetic state) has not been previously reported.

and incommensurate ordering in the form of spin excitations which abruptly shift from the incommensurate $\mathbf{q}_{inc} \approx [0.45, 0, 0.5]$ to the commensurate wavevector $\mathbf{q}_{AFM} = [1/2, 0, 1/2]$ when passing below the Néel temperature T_N (see Fig. 1). We interpret this unusual behavior in terms of a lock-in transition driven by crystalline anisotropy, which stabilizes bicollinear order.

The INS measurements were performed on a single crystal of $\text{Fe}_{1.08}\text{Te}$ with volume ≈ 0.1 cc, mass ≈ 2 g, and mosaic spread 2° . The sample was grown by the Bridgman technique, and the excess iron content was determined by Patterson refinement of single-crystal x-ray diffraction data to be $y = 0.08$. The Néel temperature was defined as the steepest slope of the magnetic Bragg peak intensity with temperature, and was found to be $T_N = 67.5$ K, consistent with other reports [7–9] for this value of y . The crystal structure at room temperature is tetragonal (space group 129, $P4/nmm$) with lattice constants $a = b = 3.823(3)$ Å and $c = 6.282(6)$ Å. Although this compound becomes monoclinic (space group 11, $P2_1/m$) at low temperature [10], the primary effect is a shift of the Te atoms within the unit cell [4]; the rotation of the c -axis away from 90° is quite small, and amounts to a broadening of certain Bragg peaks (see Fig. 2b), so we describe the measurements in the tetragonal [HLL] notation.

The neutron measurements were performed on the 1T1 triple-axis spectrometer at the Laboratoire Léon Brillouin, Saclay, France. The sample was mounted in a standard duplex cryostat (base temperature $T = 11$ K) in the [H0L] plane. The measurements were done with vertically and horizontally focusing PG crystals as monochromator and analyzer, respectively. A graphite filter was used to reduce $\lambda/2$ contamination. The scans were performed using a fixed final wavevector of $k_f = 2.662$ Å ($E_f = 14.7$ meV), corresponding to an energy resolution of 0.8 meV at the elastic line. Fitting was done using the Fityk program [11]. All constant- \mathbf{q} scans were fit with a background function (either constant or linear) and Gaussians for the peaks. Elastic scans were fit with a constant background and Voigt profile.

We measured inelastic and elastic magnetic scattering from our sample near the \mathbf{q}_{AFM} point, obtaining a detailed picture of the evolution of the magnetic order, the crystal structure, and the magnetic excitations as a function of temperature in the vicinity of the first-order phase transition from the high-temperature paramagnetic to the low-temperature AFM phase.

Figure 1 shows constant-energy scans, at $E = 6$ meV, along $[H, 0, 1/2]$ above and below T_N . At 50 K the peak is commensurate and comparable in width to the resolution function, whereas at 70 K it is broad and incommensurate.

Figure 2a details the peak scattering intensity at 2 meV, which is well below the low-T spin gap, taken along the $[H, 0, 1/2]$ -direction. This is plotted together with

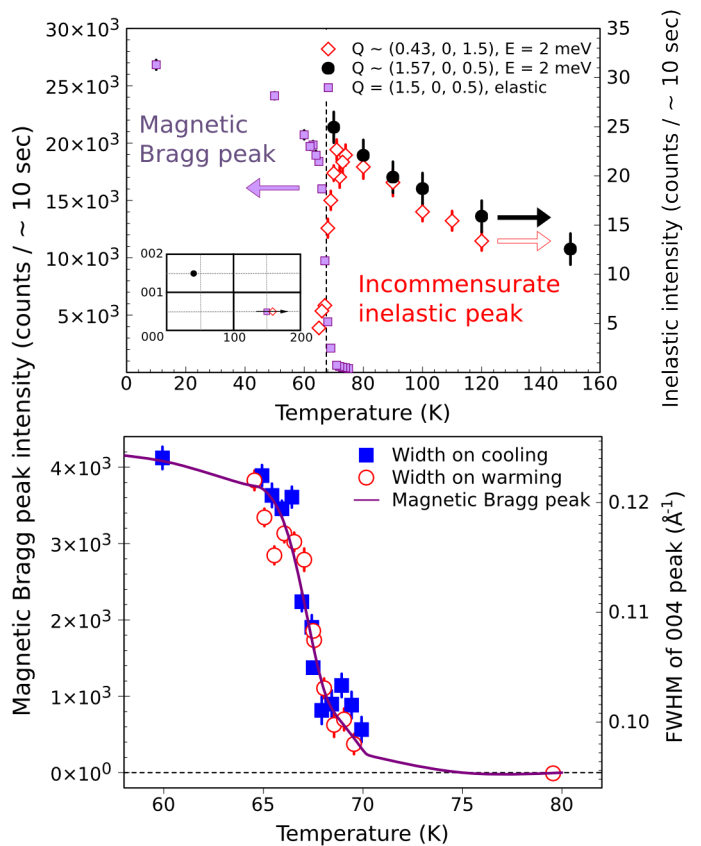


FIG. 2. (color online) Temperature dependence of the magnetic and structural behavior. (a) Peak intensities of the incommensurate magnetic excitation and the $[1.5, 0, 0.5]$ magnetic Bragg peak as a function of temperature. Inset: map of reciprocal space, showing the locations of the scans. (b) Width of the $[0, 0, 4]$ nuclear Bragg peak (an indicator of monoclinic splitting) as a function of temperature, showing the structural transition at 67.5 K. This is together plotted with the intensity of the $[2.5, 0, 0.5]$ magnetic Bragg peak, demonstrating the close coincidence between the structural and magnetic transitions.

the temperature dependence of the magnetic Bragg peak. The phase transition at 67.5 K is clearly evident: the intensity at 2 meV builds up on cooling towards the phase transition, then drops abruptly as the spin gap opens and the magnetic Bragg peak appears. The rapid increase of magnetic intensity is consistent with a first-order phase transition. We also measured the temperature dependence of the mosaic of the $[004]$ lattice reflection, which is proportional to the amount of the monoclinic distortion. Figure 2b demonstrates that the magnetic transition is concurrent with the structural phase transition to the monoclinic phase.

Figure 3 shows $S(q, \omega)$, and summarizes the energy- and wavevector-dependence of the magnetic inelastic scattering above and below T_N . Above T_N it is incommensurate, broad, and ungapped. Below T_N it is commensurate, narrow, and gapped. Both have nearly

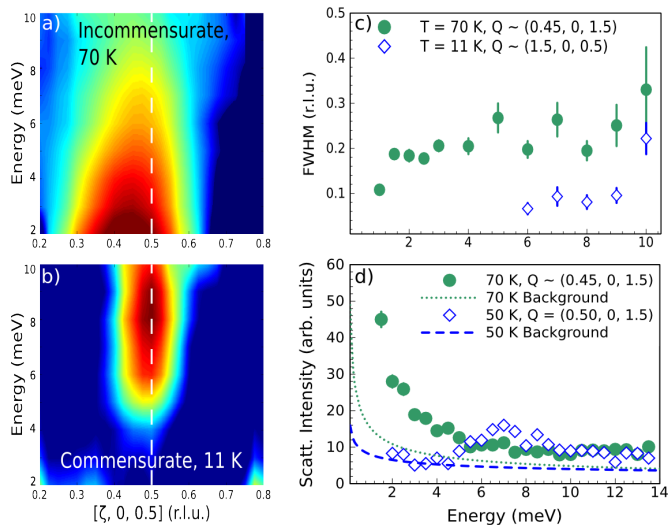


FIG. 3. (color online) Energy dependence of the spin excitations. **(a,b)** $S(q, \omega)$ at $T = 70$ K **(a)** and 11 K **(b)**. The data have been smoothed and background-subtracted. Intensity is plotted on a logarithmic scale (arb. units). **(c)** Linewidths of the incommensurate (solid green circles) and commensurate (open blue diamonds) peaks, as a function of energy. **(d)** Constant- Q scans taken at the center of the incommensurate and commensurate spin excitations.

vertical dispersion within the experimental uncertainty.

The temperature dependence of the signal with L is shown in Fig. 4. The magnetic scattering at 2 meV is nearly absent at 65 K, because of the spin gap opening at the phase transition. Upon heating in the paramagnetic phase, the signal broadens along the L -direction, although the integrated intensity stays roughly the same. The signal broadens only slightly in the H -direction (not shown). Based on this observation, we conclude that the buildup of intensity in H -integrated scans at 2 meV towards T_N shown in Fig. 2 results from an increase in the magnetic correlation length along the c -axis, as opposed to an increase of total scattering.

The most important feature of the observed behavior is that incommensurate fluctuations give rise to commensurate order, or more generally, fluctuations appear at one wavevector while ordering occurs at another. Furthermore, the *entire* accessible fluctuation spectrum shifts from being centered at $h \approx 0.45$ to $h = 0.5$, not just the low-energy part. Thus we can rule out a mechanism based on different energy scales, such as the strong energy scale determining the fluctuation wavevectors and the weak one determining the ordering wavevector (such a mechanism has been seen in layered antiferromagnets, which have 2D fluctuations controlled by J_{\parallel} and 3D order controlled by J_{\perp}). Rather, this behavior is similar to the phase transition in $\text{La}_{3/2}\text{Sr}_{1/2}\text{MnO}_4$, in which the buildup of ferromagnetic fluctuations is interrupted by orbital ordering accompanied by AFM order [12].

Existing theories do not provide a cromulent explanation for this behavior. According to the orbital scheme as discussed, for example, in Ref. [13], in the tetragonal phase the highest energy electron can occupy either d_{xz} or d_{yz} , orbitals which are otherwise empty. This orbital degeneracy implies that the entire spin system is free to rotate in the x - y plane with no in-plane anisotropy. In such a model, the bicollinear spin order results from a combination of anisotropic exchange and the biquadratic spin interaction. However, the predicted spin wave dispersion is inconsistent with the large spin gap that we and others have observed [8, 9]. Ma et al. [14] have found that DFT finds the lowest-energy *commensurate* phase to be bicollinear, even when the lattice is tetragonal. They did not calculate whether incommensurate ordering is more favorable than commensurate (DFT requires calculations using large supercells to understand the competition between commensurate and incommensurate order).

Our results (as well as those of previous experiments) may be captured by a simple model [15], in which the spin rotation symmetry is explicitly broken by the single-ion anisotropy. The low-temperature monoclinic phase features both a orthorhombic distortion with shortening along the b -axis, as well as a monoclinic shearing of the Te-planes along the a -axis. Together these distortions break the symmetry along the a - and b -axes. Thus the degeneracy between the d_{xz} and d_{yz} orbitals is removed, and the crystal field environment becomes anisotropic.

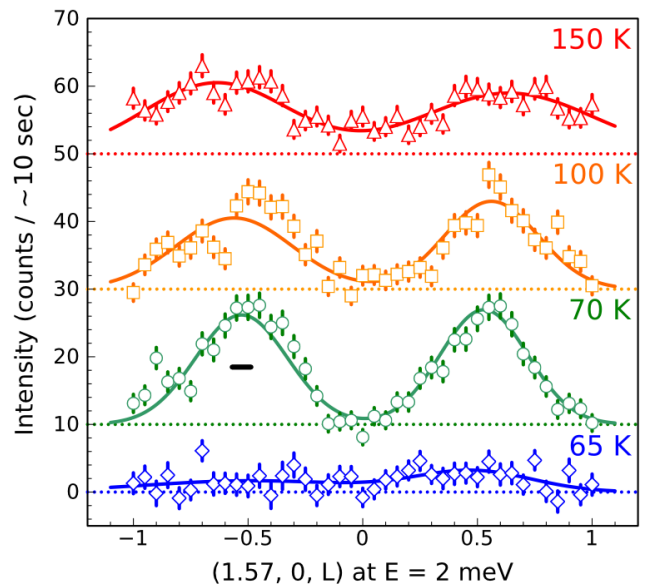


FIG. 4. (color online) Scans along the c -axis direction. The black horizontal bar shows the estimated FWHM of the resolution function. The integrated intensity is approximately constant for temperatures above T_N , indicating that the number of spins is constant, but the correlation length decreases with T .

This anisotropy locks the spins in the b^* direction and opens a gap in the spin-wave spectrum (in agreement with experiments). In the tetragonal or orthorhombic phase with incommensurate magnetic order, the degeneracy between the d_{xz} and d_{yz} orbitals has not been lifted.

Fig. 5 shows a schematic of the energy as a function of the ordering wavevector, $\mathbf{q}_{\text{ordering}}$, and illustrates the competition between the high-temperature incommensurate paramagnetic and low-temperature commensurate magnetic states. In the tetragonal phase the interactions between the electrons favor an incommensurate phase whose wavevector is not too far from $[1/2, 0, 1/2]$. This is represented by a dotted parabola on the energy vs. $\mathbf{q}_{\text{ordering}}$ plot, which has a minimum at an incommensurate wavevector. Here we are not concerned with exactly why the system wants to choose such an incommensurate wavevector, although such a wavevector

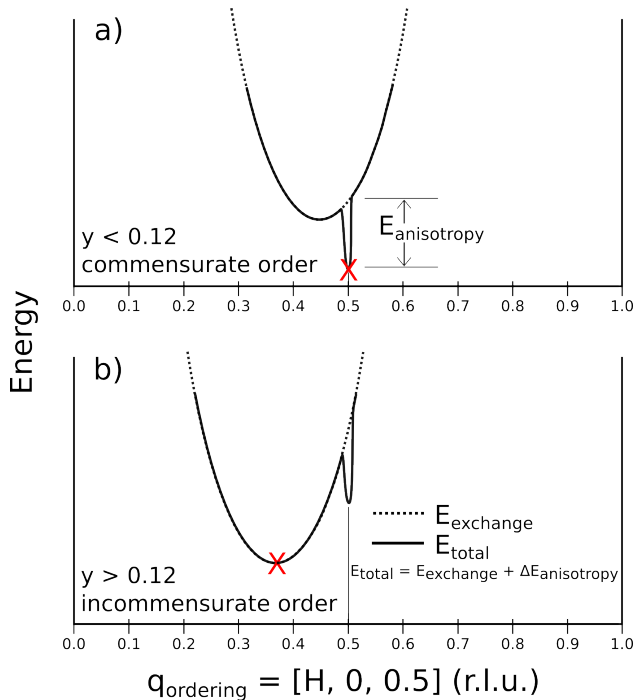


FIG. 5. (color online) Schematic of the magnetic energy in Fe_{1+y}Te at zero temperature as a function of the ordering wavevector, for two values of the excess iron concentration y . The exchange energy, E_{exchange} , is represented as a parabola (dashed line); the structural anisotropy at the commensurate wavevector lowers the total energy, E_{total} , further by $\Delta E_{\text{anisotropy}}$. The system always settles at the global energy minimum, marked with an “X”. (a) For values of $y < 0.12$, the minimum of E_{exchange} is close to the commensurate wavevector, and so the global minimum is at the *commensurate* position. Above T_N the anisotropy well becomes filled, thus spin fluctuations appear at $\mathbf{q}_{\text{inc}} = [0.45, 0, 0.5]$, the exchange energy minimum. (b) For $y > 0.12$, the energy minimum for E_{exchange} is far from the commensurate position, which puts the global minimum at an *incommensurate* wavevector near $\mathbf{q}_{\text{inc}} = [0.38, 0, 1/2]$ [4, 9].

is probably easy to achieve, given the interplay between different exchange, superexchange, and double-exchange pathways [13]. However, the commensurate wavevector is special, because it allows the system to lower energy by an amount $\Delta E_{\text{anisotropy}}$ through the monoclinic lattice distortion, which in turn allows the magnetic order to align the moments according to the spin anisotropy. Thus E_{total} has a dip at the commensurate \mathbf{q} . If that dip is close to the minimum of the exchange interactions, then it will be the global minimum, and the ground state will become bicollinear through the monoclinic distortion (this distortion is probably cooperative, since J_1 and J_2 will split under the monoclinic and orthorhombic distortions, respectively). Thus the incommensurate fluctuations we observe in the paramagnetic phase are the precursor to ordering, and in the absence of the lock-in transition the system would eventually order at this incommensurate wavevector. At temperatures greater than the anisotropy gap (≈ 6 meV, corresponding to 69 K), the spins are thermally excited above the gap, and the advantage it provides to the commensurate order disappears.

This lock-in scenario is expected to take place in the low-Fe doping regime. At the critical excess iron concentration $y \approx 0.12$, the system enters a mixed-phase regime [16, 17], consistent with two minima (at the commensurate and incommensurate wavevectors). With further y -doping, the system becomes single-phase, and the incommensurability increases rapidly to $\mathbf{q}_{\text{inc}} = [0.38, 0, 1/2]$ [16], while the orthorhombic distortion simultaneously decreases [4], which suggests the reduction of anisotropy. This can be understood as a doping-driven (as opposed to temperature-driven) classical commensurate-incommensurate transition [15], in which the cost of the exchange energy required to form the bicollinear phase is greater than the energy gained by the anisotropy gap (see Fig. 5). This commensurate-incommensurate transition is expected to be continuous and can be interpreted as the condensation of the domain walls (or solitons) of the commensurate state. One consequence of the doping-driven commensurate-incommensurate transition is that at finite temperature a soliton liquid is expected to occur between the commensurate state (soliton vacuum) and the incommensurate state (soliton line crystal) [18, 19]. Thus for intermediate values of y , examining the fluctuations just above T_N should show the dependence of the preferred ordering for the electronic system as a function of doping.

To conclude, we have observed clear signatures of a competition between commensurate and incommensurate magnetism in a well-characterized sample of $\text{Fe}_{1.08}\text{Te}$. We find incommensurate fluctuations above T_N , which give way to commensurate order below T_N with a gap in the excitation spectrum. This behavior, as well as other previously unexplained observations, can be understood in terms of a lock-in transition induced by

the spin anisotropy gap which is present in the monoclinic bicollinear phase and absent in the tetragonal phase.

D.P and D.R. were supported by the DOE, Office of Basic Energy Sciences under Contract No. DE-SC0006939. The extended visit of D.P. to KIT, during which part of this work was performed, was supported by the International Institute for Complex Adaptive Matter, and by NSF grants DMR-0847782, DMR-0820579, and DMR-0844115. L.R. was supported through NSF through grant No. DMR-1001240. G. C. was supported by the David and Lucile Packard Foundation. The authors are grateful to I. Mazin for valuable discussions, and to J. L. Niedziela for critical reading of the manuscript.

* dan.parshall@colorado.edu

- [1] Y. Kamihara, T. Watanabe, M. Hirano, and H. Hosono, *Journal of the American Chemical Society* **130**, 3296 (2008), <http://pubs.acs.org/doi/pdf/10.1021/ja800073m>.
- [2] J. Paglione and R. L. Greene, *Nature Physics* **6**, 645 (2010).
- [3] I. I. Mazin, D. J. Singh, M. D. Johannes, and M. H. Du, *Physical Review Letters* **101**, 057003 (2008).
- [4] W. Bao, Y. Qiu, Q. Huang, M. A. Green, P. Zajdel, M. R. Fitzsimmons, M. Zhernenkov, S. Chang, M. Fang, B. Qian, E. K. Vehstedt, J. Yang, H. M. Pham, L. Spinu, and Z. Q. Mao, *Physical Review Letters* **102**, 247001 (2009).
- [5] A. Subedi, L. Zhang, D. Singh, and M. Du, *Physical Review B* **78**, 134514 (2008).
- [6] Y. Xia, D. Qian, L. Wray, D. Hsieh, G. F. Chen, J. L. Luo, N. L. Wang, and M. Z. Hasan, *Phys. Rev. Lett.* **103**, 037002 (2009).
- [7] T. J. Liu, J. Hu, B. Qian, D. Fobes, Z. Q. Mao, W. Bao, M. Reehuis, S. A. J. Kimber, K. Prokeš, S. Matas, D. N. Argyriou, A. Hiess, A. Rotaru, H. Pham, L. Spinu, Y. Qiu, V. Thampy, A. T. Savici, J. A. Rodriguez, and C. Broholm, *Nature Materials* **9**, 718 (2010).
- [8] O. Lipscombe, G. Chen, C. Fang, T. Perring, D. Abernathy, A. Christianson, T. Egami, N. Wang, J. Hu, and P. Dai, *Physical Review Letters* **106**, 057004 (2011).
- [9] C. Stock, E. E. Rodriguez, P. Zavalij, M. A. Green, and J. A. Rodriguez-Rivera, arXiv:1103.1811 (2011), 1103.1811..
- [10] S. Li, C. de la Cruz, Q. Huang, Y. Chen, J. W. Lynn, J. Hu, Y.-L. Huang, F.-C. Hsu, K.-W. Yeh, M.-K. Wu, and P. Dai, *Physical Review B* **79**, 054503 (2009).
- [11] M. Wojdyr, *Journal of Applied Crystallography* **43**, 1126 (2010).
- [12] D. Senff, O. Schumann, M. Benomar, M. Kriener, T. Lorenz, Y. Sidis, K. Habicht, P. Link, and M. Braden, *Phys. Rev. B* **77**, 184413 (2008).
- [13] A. M. Turner, F. Wang, and A. Vishwanath, *Physical Review B* **80**, 224504 (2009).
- [14] F. Ma, W. Ji, J. Hu, Z.-Y. Lu, and T. Xiang, *Physical Review Letters* **102**, 177003 (2009).
- [15] S. Choi, G. Chen, and L. Radzihovsky, unpublished.
- [16] E. E. Rodriguez, C. Stock, P. Zajdel, K. L. Krycka, C. F. Majkrzak, P. Zavalij, and M. A. Green, *Physical Review B* **84**, 064403 (2011), 1012.0590v1.
- [17] I. A. Zaliznyak, Z. J. Xu, J. S. Wen, J. M. Tranquada, G. D. Gu, V. Solovyov, V. N. Glazkov, A. I. Zheludev, V. O. Garlea, and M. B. Stone, arXiv:1108.5968v1.
- [18] S. N. Coppersmith, D. S. Fisher, B. I. Halperin, P. A. Lee, and W. F. Brinkman, *Physical Review B* **25**, 349 (1982).
- [19] V. Pokrovsky and et al., *Solitons*, edited by S. Trullinger and et al. (North Holland, Amsterdam, 1986) pp. 71–127.